

Non-local topographic influences on deep convection: An idealized model for the Nordic Seas

Michael A. Spall

MS#21, 360 Woods Hole Road, Woods Hole, MA 02543, United States

ARTICLE INFO

Article history:

Received 22 May 2009

Received in revised form 26 October 2009

Accepted 29 October 2009

Available online 1 November 2009

Keywords:

Nordic Seas
Thermohaline circulation
Baroclinic instability
Mesoscale eddies
Convection

ABSTRACT

Issues relevant to the water mass transformation and circulation in the Nordic Seas are explored using a series of idealized numerical model calculations. The essential aspects of the model configuration are: a marginal sea with two sub-basins separated by a ridge; a sill separating the marginal sea from the open ocean; a region of sloping topography surrounding the marginal sea; surface heat loss; and eddy-resolving physics. A calculation with enhanced topographic slope along the eastern boundary, as is found in the Lofoten Basin, produces a hydrography and circulation that are similar to that observed in the Nordic Seas, including two poleward warm currents, a mid-depth thermocline in the eastern basin (the model's Lofoten Basin), and deep convection in the western basin (the model's Greenland Sea). It is shown that the key elements to the mid-ocean poleward warm current and the mid-depth thermocline in the eastern basin are: an asymmetry in the eddy heat flux from the boundary into the basin interior, here related to a region of steep bottom topography that makes the eastern boundary current more unstable than the western boundary current, and a mid-ocean ridge that partially, but not completely, inhibits exchange between eastern and western basins. This exchange can take place by baroclinic eddy fluxes or by flow through deep gaps in the ridge. The basin-scale hydrography and circulation in this idealized Nordic Seas are controlled to a large degree by eddy fluxes, which are themselves strongly influenced by regional features of the bottom topography that are located far from the convection sites.

© 2009 Elsevier Ltd. All rights reserved.

1. Introduction

In the northern North Atlantic, poleward flowing warm waters are cooled by the atmosphere, leading to the formation of dense water masses that eventually sink and return equatorward. This water mass transformation, closely associated with the Atlantic Meridional Overturning Circulation (AMOC), occurs primarily in two regions – the North Atlantic subpolar gyre and the Nordic Seas. Much attention has been paid to the water mass transformation and deep convection that occurs in the Labrador Sea in the subpolar gyre and the Greenland Sea region of the Nordic Seas (see review by Marshall and Schott (1999)). This is at least in part due to the early notion that the dense overflows were directly linked to waters formed in such deep convection regions (e.g. Killworth, 1983; Aagaard et al., 1985). However, recent studies suggest that the gradual transformation of waters along the advective pathways around the regions of deep convection plays a more important role than these deep convection sites in both the AMOC and the heat budget (Mauritzen, 1996a,b; Isachsen et al., 2007; Eldevik et al., 2009). Recent theoretical studies indicate that the boundary currents are dynamically linked to regions of deep convection and that the waters that exit

convective basins are composed of waters from both deep convection sites and cyclonic boundary currents (Spall, 2004; Straneo, 2006; Chanut et al., 2008), so it is difficult to address transformation without considering both regions together.

Much of the water mass transformation that occurs in the Nordic Seas takes place in the Lofoten Basin (Isachsen et al., 2007). Warm water of Atlantic origin flows northward through this basin in two main branches, the inner Norwegian Atlantic Current (iNwAC), which follows the continental slope along the west coast of Norway, and the outer Norwegian Atlantic Current (oNwAC), which flows along the Mohn and Knipovich Ridges (Orvik and Niiler, 2002; Fig. 1). This partition is evident by the hydrographic section taken as part of the Circulation And Thermohaline Structure (CATS) program (Fig. 2). There is a strong horizontal temperature gradient over the Mohn Ridge, separating the warmer waters of the Lofoten Basin from the colder waters in the Greenland Sea. Similar gradients are found for salinity, with more saline Atlantic waters found in the Lofoten Basin. The sloping isotherms indicate a geostrophic upper ocean flow northwards over both the ridge and along the eastern boundary. The region between these two currents is filled with warm, salty Atlantic Water down to approximately 800 m depth. The spreading of this warm water over the spatial extent of the Lofoten Basin results in a larger net heat loss to the atmosphere than if the warm

E-mail address: mspall@whoi.edu

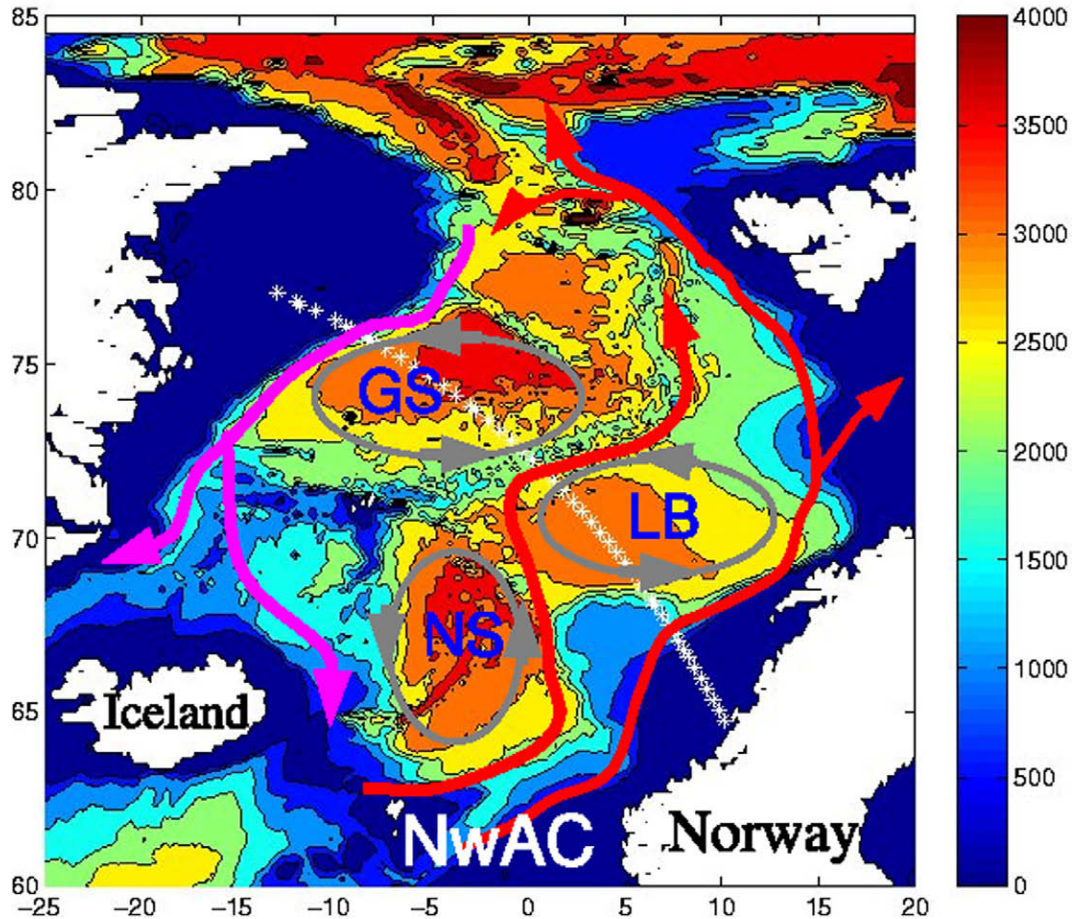


Fig. 1. Schematic of the major currents with bottom topography for the Nordic Seas. Red arrows indicate the two northward branches of the NwAC, the magenta arrows indicate the southward flowing transformed waters that enter the North Atlantic, and the grey pathways mark cyclonic recirculation gyres in each of the sub-basins. The locations of the stations in the CATS hydrographic section (Fig. 2) are marked by white asterisks. LB: Lofoten Basin, GS: Greenland Sea, NS: Norwegian Sea. (For interpretation of the references to color in this figure legend, the reader is referred to the web version of this paper.)

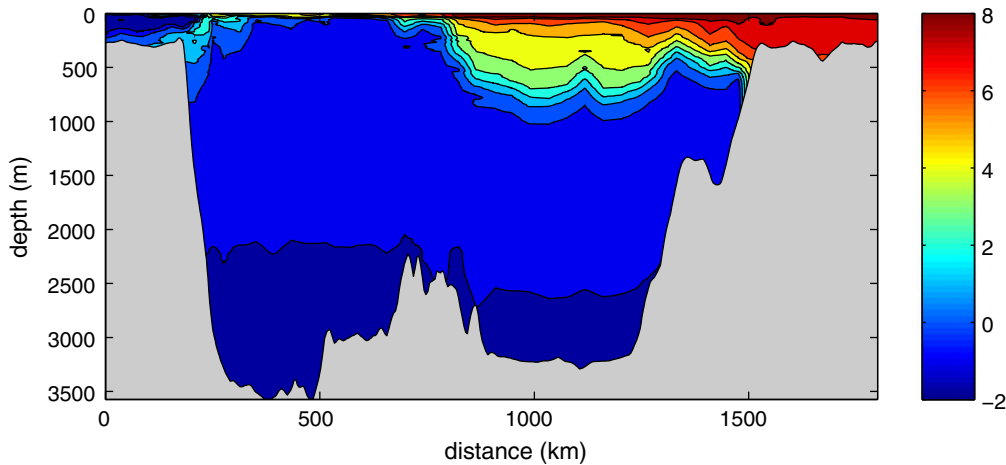


Fig. 2. Potential temperature from the CATS hydrographic section taken during the summer of 1999 (Oliver and Heywood, 2003; station locations indicated in Fig. 1). Warm Atlantic water with a mid-depth local minimum in stratification fills the upper ocean within the Lofoten Basin. The topography is interpolated from the GEBCO data base, but the actual topography taken from the cruise shows the Mohn Ridge extending to almost 1000 m depth (Oliver and Heywood, 2003).

water remained more confined to a narrow boundary current, as for the Labrador Sea. The warm water in the basin interior appears to be provided by eddies shed from the iNwAC (Poulain et al., 1996; Köhl, 2007). Even though the heat loss here is large, this source of warm water limits convection to only 500–800 m depth, much less than is found in the Greenland Sea (Nilsen and Falck, 2006). The stratifica-

tion has a local minimum around 500 m depth and a local maximum at around 800 m depth. The abyssal Lofoten Basin is very weakly stratified and cold. The southward flowing boundary current adjacent to Greenland is much colder than the northward flowing Atlantic Waters and also more weakly stratified as a result of heat loss and convection to the north of this section.

While this general description of the circulation through the Nordic Seas has been known for some time, important basic questions remain. Why does the NwAC flow northward in two branches? There is clearly a topographic constraint because both fronts lie over regions of sloping topography. Orvik (2004) argues that the deepening of the Atlantic Water is a result of a deep counter current adjacent to the Mohn Ridge. However, this is more of a consistency constraint and does not explain why the Atlantic Water spreads over the Lofoten Basin, why there are two branches of the NwAC, or why a deep counter current exists. A related question is why does convection penetrate to great depths in the Greenland Sea and only to intermediate depths in the Lofoten Basin even though the heat loss in the Lofoten Basin is larger? The idealized buoyancy-forced models of Walin et al. (2004) and Spall (2004) produce cyclonic boundary currents and regions of deep convection, but do not produce a mid-depth thermocline or multiple poleward branches.

The present study aims to address these general questions with a set of very idealized numerical model calculations. Although the issues are motivated by the Nordic Seas, the model has been simplified considerably compared to this very complex region. However, the model retains several key elements of the Nordic Seas, including: a sill separating the marginal seas from the warm low latitude oceans; a mid-ocean ridge separating the marginal sea into eastern and western sub-basins; variable topography around the perimeter of the marginal sea; nonlinearities and mesoscale eddies; and surface buoyancy loss. The primary goal here is to better understand how various aspects of the bottom topography and eddy fluxes can influence the mean circulation, water mass transformation, and deep convection in buoyancy-forced marginal seas.

2. An idealized numerical model for the Nordic Seas

The model used in this study is the hydrostatic version of the MIT-gcm (Marshall et al., 1997). The model solves the primitive equations on a Cartesian grid in the horizontal and on depth levels in the vertical. The horizontal grid resolution is 5 km and has 20 levels in the vertical with spacing ranging from 25 m near the surface to 400 m at the deepest level. Density is represented by temperature only with a thermal expansion coefficient of $0.2 \text{ kg m}^{-3} \text{ C}^{-1}$. Subgridscale viscous parameterization is represented by a lateral Laplacian viscosity of $10 \text{ m}^2 \text{ s}^{-1}$ and a lateral biharmonic viscosity of $10^9 \text{ m}^4 \text{ s}^{-1}$. There is no explicit lateral mixing of temperature. Vertical mixing of momentum and temperature are provided by a Laplacian mixing with coefficient $10^{-5} \text{ m}^2 \text{ s}^{-1}$. Convective plumes are parameterized by increasing the vertical mixing coefficient for temperature to $1000 \text{ m}^2 \text{ s}^{-1}$ for statically unstable profiles.

The basin consists of a circular marginal sea 3000 m deep separated from an “open ocean” to the south by a 1200 m deep sill (Fig. 3). The standard calculation has a region of sloping topography encircling the marginal sea that gets steeper along the eastern boundary (motivated by the region of steep topography along the eastern side of the Lofoten Basin, Fig. 1). The bottom slope between 500 m and 2000 m depth along the eastern Lofoten Basin (between 10°E and 15°E) is approximately 0.09, about a factor of 3 steeper than that found along the western boundary of the Greenland Sea between 12°W and 5°W . There is also a 1200 m deep ridge that separates the marginal sea into two sub-basins, mimicking the Mohn and Knipovich ridge system. The model is forced by imposing a uniform heat loss north of the sill¹ of 150 W m^{-2} for a period

of 120 days and then no surface forcing for a period of 240 days, repeating every 360 days, giving an annual mean heat loss of 50 W m^{-2} . The seasonal cycle is not crucial to the general results described here, a similar mean hydrography and circulation are found for steady heat loss at the annual mean strength. A source of heat is provided to balance this cooling by restoring the temperature towards a uniform stratification with $N^2 = 2 \times 10^{-6} \text{ s}^{-2}$ and a surface temperature of 10°C with time scale 20 days in the “open ocean”, indicated in Fig. 3 by the region within the white dashed line. This is very similar to the configuration used by Spall (2004), except that now a sill, ridge, and variable topographic slope are considered. The straits modeled here are wide and deep enough that hydraulic controls do not arise, however, a similar approach can be used for hydraulically controlled exchanges (e.g. Pratt and Spall, 2008). The model is initialized with the open ocean stratification and integrated for a period of 150 years. The model takes about 75 years to arrive at a statistically equilibrated state. Mean quantities discussed will be taken over the final 75 years of integration.

The mean temperature and horizontal velocity at 12.5 m depth are shown in Fig. 4. Warm water flows into the marginal sea over the sill and most follows the eastern boundary cyclonically around the basin. There is also transport directly northward over the mid-basin ridge, starting along the eastern side of the ridge and shifting towards the western side as it extends northward.² There is a cyclonic recirculation in the interior of both the eastern and western basins. The eastern basin is much warmer than the western basin, resulting in a strong baroclinic front located over the mid-ocean ridge. The velocity along the eastern boundary is of $O(15 \text{ cm s}^{-1})$ and the velocity over the ridge is somewhat stronger, approximately 25 cm s^{-1} .

A vertical section taken along 630 km latitude shows more clearly the horizontal and vertical structure of the currents in each basin (Fig. 5). Relatively warm water fills the eastern basin down to approximately 1500 m, close to the depth of the mid-ocean ridge and sill. There is a region of minimum stratification centered around 700 m depth, flanked above and below by increased stratification. The abyss in the eastern basin is also weakly stratified and cold. The warmest water is concentrated near the eastern boundary, with a secondary maximum in sea surface temperature near the mid-ocean ridge. The western basin is weakly stratified throughout most of the interior, with the exception of the upper few hundred meters. The eastern boundary current has a significant barotropic component, while the northward flow over the ridge is strongly baroclinic. There is also a weaker cyclonic circulation in the eastern basin with southward flow just to the east of the ridge. The southward flowing boundary current in the western basin is approximately 25 cm s^{-1} , but is much less stratified than the northward flowing eastern boundary current as a result of convection in the boundary current.

This section has several similarities with the schematic shown in Fig. 1 and the CATS section across the Lofoten and Greenland Basins. The primary features of the observed hydrography and circulation are: northward flow along the eastern boundary and Mohn and Knipovich Ridge system; southward flow along the western boundary, cyclonic circulations in both basins; thick layer of warm water in the eastern basin; and mid-depth local minimum in stratification in the eastern basin. That the eastern boundary current is more barotropic than the ridge current in the model is consistent with Orvik et al. (2001) and Oliver and Heywood (2003), although the former reference is located further upstream in the Norwegian Basin. There is evidence of southward flow near the bottom along the Mohn Ridge indicating a cyclonic circulation in the Lofoten

¹ A calculation in which the surface heat flux is provided by restoring the model upper level temperature towards a prescribed temperature uniform in space produces a very similar result. The specified heat flux boundary condition is used to ensure that any differences between the eastern and western basins are not due to different surface heat fluxes.

² This westward shift is a result of the Reynolds stress divergence due to eddy formations along the ridge current.

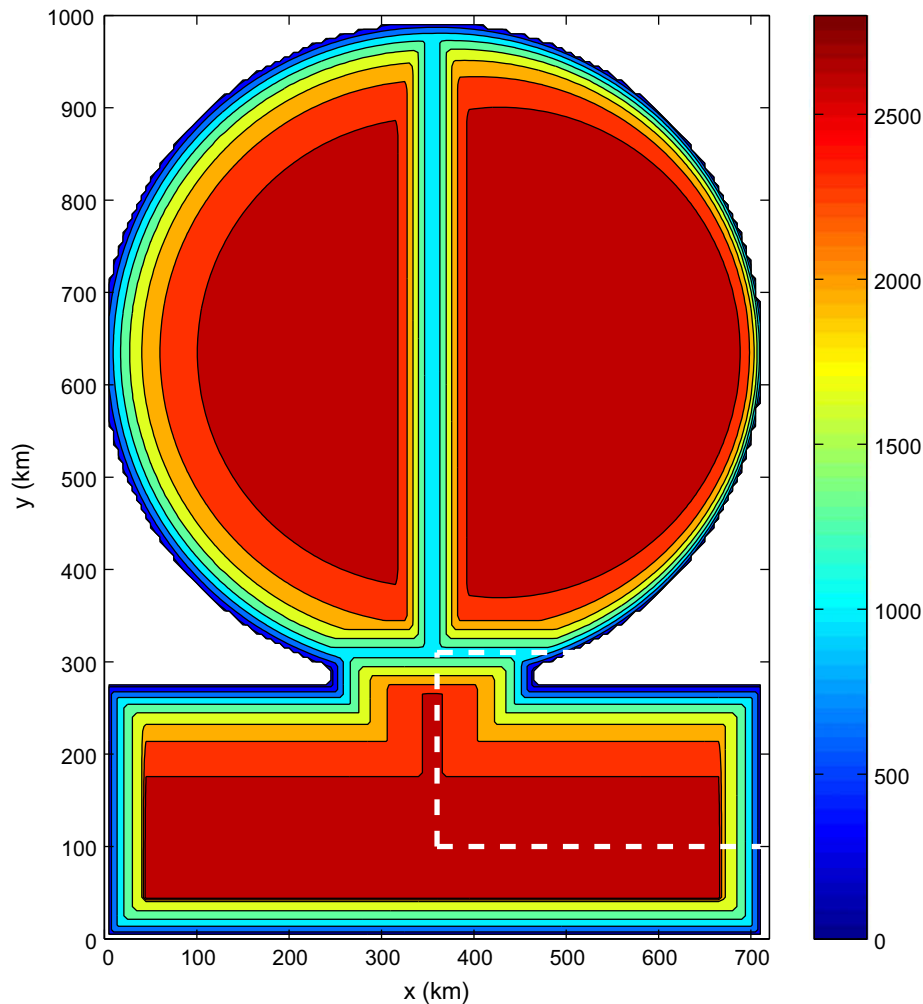


Fig. 3. The model domain and bottom topography. The model is forced with spatially uniform cooling over the marginal sea (north of the sill) and a restoring of temperature to a uniform stratification within the region marked by the white dashed line.

Basin, as discussed by Orvik (2004), surface drifters do not show evidence of southward flow extending to the surface to the east of the oNwAC (e.g. Orvik and Niiler, 2002), so the cyclonic circulation in the model appears to be too barotropic in this region.

The process of winter convection and restratification provides some clues regarding the asymmetric hydrography and circulation in this calculation. The mixed layer depth (defined as the depth at which the temperature is $0.1\text{ }^{\circ}\text{C}$ less than the surface temperature, the general result is not very sensitive to this choice) is shown in Fig. 6 at the end of the cooling period in year 95 (this is typical of any year). The primary pathways into the marginal sea are marked by the shallow mixed layer depths along the eastern boundary and over the mid-ocean ridge. These are the two regions that are first restratified at the end of winter. The mixed layer depth in the eastern basin extends down to mid-depths, between 750 m and 1000 m, and covers much of the sub-basin interior. Convection in this basin rarely exceeds 1000 m. The mixed layer depth in the western basin extends all the way to the bottom in places. These regions of deepest mixing are confined to smaller areas due to both inhomogeneities in the stratification at the beginning of winter and lateral heat advection in the form of eddies and filaments during winter.

The depth of convection and spin-up of the basins are indicated by the annual mean temperature at central points in the eastern and western basins shown in Fig. 7. Both basins convect deeply,

reaching the bottom, over the first 20 years. The interior of each basin continues to get more dense until eddy fluxes from the boundary provide enough heat to balance the surface cooling (Spall, 2004). This happens in the eastern basin between years 30 and 40, while in the western basin the influx of warm water is delayed another 10–20 years. The band of weakly stratified water centered around 700 m is evident in the eastern basin, as is the enhanced stratification near 1200 m that isolates the abyss. The western basin is colder and has much weaker stratification over most of the water column. There is a hint of low frequency variability in the heat content and depth of convection in the western basin (warm anomalies during years 45–70 and 90–110), although there is no corresponding signal in the eastern basin.

The restratification process is indicated by the upper level temperature 80 days after cooling ended in year 95 (Fig. 8). The warm current along the eastern boundary has developed large meanders and is shedding warm eddies into the interior. The boundary currents around the western basin and over the mid-ocean ridge show much less meandering and eddy shedding. The enhanced instability along the eastern boundary is due to the decrease in the width of the region of sloping topography. This is consistent with the enhanced eddy variability observed in the Lofoten Basin by altimeter data (Köhl, 2007) and drifters (Poulain et al., 1996). These eddies are the reason that the eastern basin is warmer than the western basin, as will be further demonstrated in the following section. This

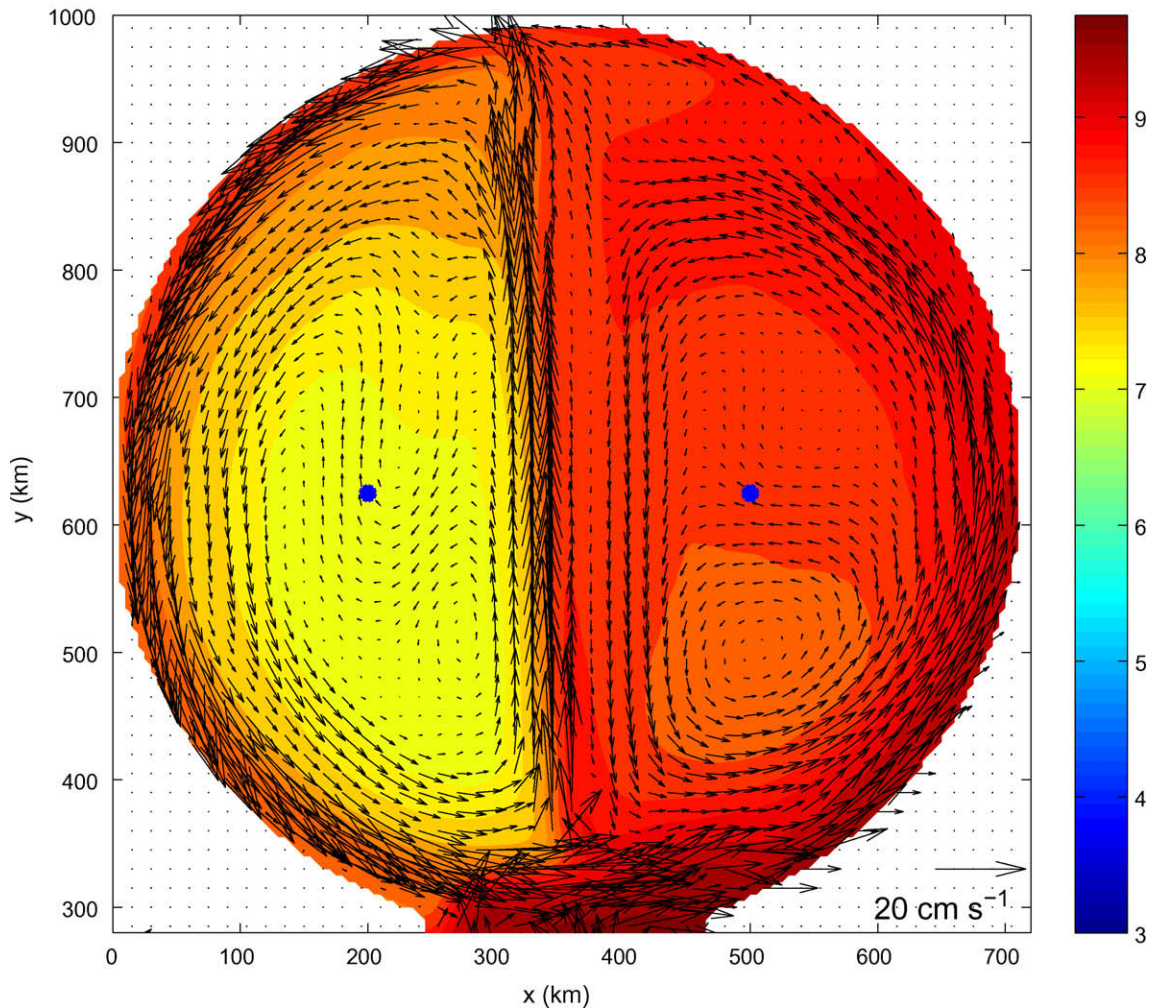


Fig. 4. Mean sea surface temperature ($^{\circ}\text{C}$) and velocity vectors (every third grid point, vector scale is indicated in lower right corner) over the final 75 years of integration for the central calculation. The blue dots in the center of the basins mark the locations of the time series in Fig. 7. (For interpretation of the references to color in this figure legend, the reader is referred to the web version of this paper.)

pathway of warm water from the eastern boundary current, into the eastern basin, and finally into the western basin over the ridge explains why the eastern basin stratifies before the western basin during spin-up (Fig. 7).

The role of steep topography in the destabilization of the boundary current is complex and, at first consideration, seems to contradict the theoretical results of Blumsack and Gierasch (1972), (hereafter BG72), who found that bottom slopes of the opposite sense to the isopycnal slope always stabilize the flow. Nonetheless, the linear quasi-geostrophic theory of BG72 does indicate that the boundary current will become more unstable as the topography steepens if the mean flow follows the topography and conserves baroclinic transport. In this case, the isopycnal slope increases over the steep topography so that the ratio of the bottom slope to the isopycnal slope remains constant (the δ parameter in BG72 and Spall, 2004) and the relative influence of topography on the linear stability is unchanged. However, the Eady growth rate for this more strongly sheared flow is larger, so perturbations are in fact more unstable. This destabilization may be mitigated by the nonlinear effect of the eddy heat fluxes reducing the isopycnal slopes as one follows the flow around the basin, but the basic finding in the model is consistent with the linear, QG theory.

The deep eastern basin is not directly reached by local convection, but there is a source of cold waters to the deepest part of the

basin, as indicated by the recurring cold waters near the bottom in Fig. 7. A synoptic section taken along 600 km latitude shows dense water spilling over the ridge into the eastern basin (Fig. 9). Such events occur intermittently in time and space along the ridge, and are related to meandering activity of the front over the mid-ocean ridge. This provides a source of dense water that fills the eastern basin from below. The local maximum in stratification near 1200 m depth is maintained by the source of low potential vorticity water in the abyss originating from convective activity in the western basin and the upper ocean low potential vorticity from convection in the eastern basin. Observations indicate that the deep Lofoten Basin contains waters that originated in the Greenland Sea (Blindheim, 1990; Oliver and Heywood, 2003).

An idealized age tracer has been inserted over the final 30 years of integration. The tracer is initially zero everywhere, maintained at zero at the surface, and increases with time in the interior. It is advected and mixed the same as temperature. It marks the average time since a water parcel has been in contact with the atmosphere. A section of this age tracer at the mid-latitude of the basin averaged over the final 2 years of model integration is shown in Fig. 10. The ventilation of the upper ocean is evident in both basins, although there are differences. The most recently ventilated waters in the western basin are confined close to the surface in the interior, while they penetrate down to about 800 m in the

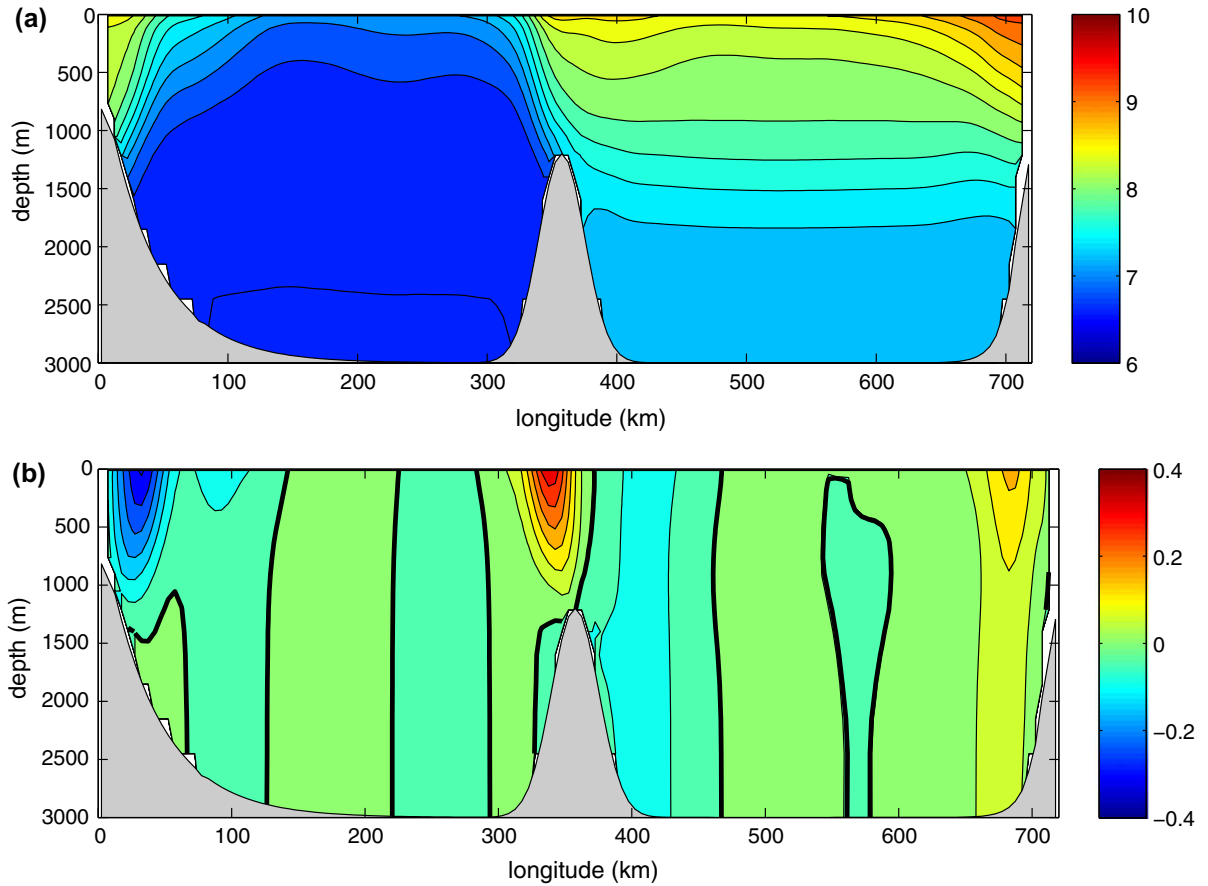


Fig. 5. Vertical section at 630 km latitude of mean (a) temperature (contour interval 0.2 °C) and (b) meridional velocity (m s^{-1} , contour interval 0.05, zero line bold) taken over the final 75 years of integration.

eastern basin. The water in the deep western basin is about 8 years old on average, while the water in the deep eastern basin is approximately 16 years old.

The deep western basin water is, on average, much older than 1 year even though there is convection to the bottom in every winter. This is because the deepest convection is isolated to a few small regions each year and the eddies rapidly mix this ventilated water with the surrounding larger volume of unventilated water. If convection reaches a given depth over a fraction ϵ of the basin, then the average age A of a water parcel at that depth in year $n + 1$ is related to the average age of the water parcel in year n by

$$A_{n+1} = (1 - \epsilon)(A_n + 1). \quad (1)$$

The age can be written explicitly for any year n , assuming that the age is zero at $n = 0$, as

$$A_n = \frac{1 - \epsilon}{\epsilon} (1 - (1 - \epsilon)^n). \quad (2)$$

It is easy to see that for $0 < \epsilon < 1$, the age for large n is simply

$$A = \epsilon^{-1} - 1. \quad (3)$$

From this, one can infer that the deepest part of the western basin is ventilated over only approximately 10% of its area each winter. This is consistent with the regions of deepest mixing found at the end of winter in Fig. 6 (convection exceeds 2000 m over 12% of the western basin). The deeper penetration of recently ventilated waters in the eastern basin (Fig. 10) results from having a larger fraction of the basin exposed to convection down to depths of 1000 m, while in the western basin much of the region has convection limited to depths less than 500 m (Fig. 6). This different behavior can be most

easily understood by recognizing that the variability in mixed layer depth (for this uniform cooling scenario) is solely a result of density anomalies at the beginning of the cooling period that result from natural variability due to eddies formed from the boundary current. The variability in mixed layer depth represents variability in heat content integrated over the depth of convection. For the eastern basin, the stratification is large at the base of the mixed layer, so small changes in mixed layer depth represent relatively large changes in integrated heat content. However, for the western basin the stratification is very weak so that small changes in heat content represent very large changes in mixed layer depth. The same warm anomaly will result in a much larger decrease in mixed layer depth in the western basin than it will in the eastern basin. Thus the variability in mixed layer depth is larger in the western basin, resulting in deep mixing over a relatively smaller portion of the basin.

The transition in age from the surface to the deep ocean is gradual in the western basin but abrupt, coincident with the mid-depth thermocline, in the eastern basin. The deep regions of strong currents over the mid-ocean ridge and western topography are less well ventilated, reflecting the lack of deep convection there, although convection does penetrate deeper along the western boundary. Convection does not penetrate deeply in the more stratified eastern boundary current, however, there is a mid-depth minimum in the age tracer on the boundary. This is a result of the baroclinic eddy exchange between the boundary current and the interior. The freshly ventilated water at approximately 800 m depth was formed in the basin interior and transported into the boundary current through baroclinic instability. The mid-depth minimum in age over much of the interior of the eastern basin is evidence of restratification of the interior due to eddy fluxes from the boundary

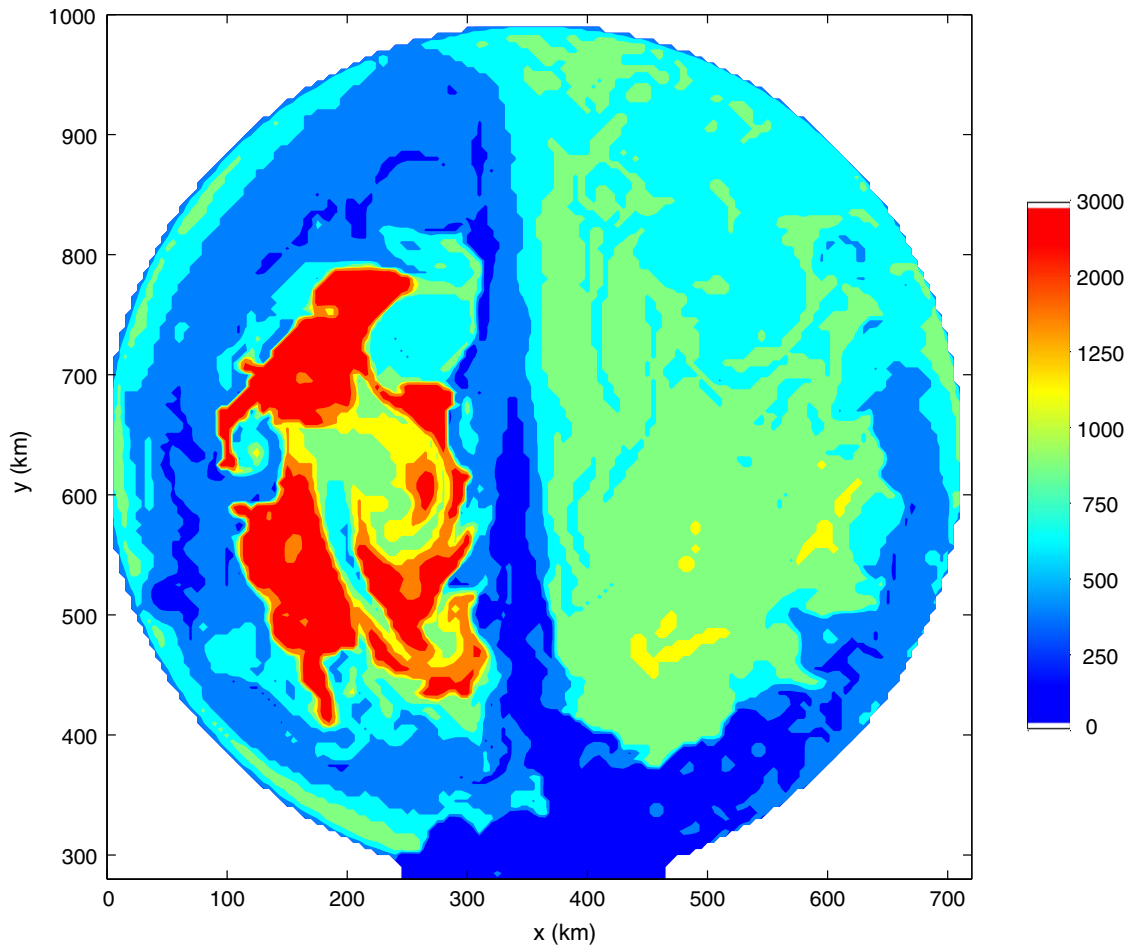


Fig. 6. Mixed layer depth (m) at the end of the cooling period in year 95.

current. The ventilation pathways into the deep eastern basin are also indicated by the relatively young waters penetrating downward along the mid-ocean ridge. The dense water mixes with the ambient water as it flows down the topography, as evidenced by the vertical tracer contours near the ridge. The mid-ocean ridge is the location of dense water boluses shown in Fig. 9.

The existence of the mid-depth thermocline in the eastern basin is a direct result of the steep topography that causes the boundary current in the eastern basin to be more unstable than the western boundary current in the western basin. Each basin loses the same amount of heat to the atmosphere, which is balanced by the eddy heat flux from the boundary currents (discussed more in the next section). The region of steep topography acts to destabilize the eastern boundary current because the horizontal scale of the current decreases with the topographic width, increasing the horizontal density gradient and the vertical shear in the velocity, thus decreasing the stability of the boundary current. Because of this, the density change between the boundary current and the interior that is required to support the lateral eddy heat flux that balances the surface cooling in the eastern basin is less than it is in the western basin. This means that the upper ocean temperature in the eastern basin must be warmer than it is in the western basin. Since the baroclinic exchange across the ridge fluxes water from the western basin into the eastern basin over the ridge, this results in an abyssal water mass in the eastern basin that must be more dense than the upper ocean in the eastern basin, resulting in a mid-depth thermocline.

A similar narrowing of the slope width is found along the eastern boundary of the Labrador Sea, and appears to result in a similar

enhancement of the boundary current instability and localization of eddy shedding (White and Heywood, 1995; Prater, 2002; Cuny et al., 2002). It has been hypothesized that these boundary current eddies play an important role in the restratification of deep convection sites in the Labrador Sea (Lilly and Rhines, 2002; Katsman et al., 2004).

2.1. Energetics

The restratification process depicted in Fig. 8 indicates the importance of lateral eddy fluxes to the seasonal cycle in this idealized convective basin. This is further demonstrated by the time mean eddy temperature flux shown in Fig. 11 at 275 m depth. Time-dependent motions are carrying heat into the interior of the eastern basin along the middle and northern portions of the eastern boundary. The heat flux into the western basin is provided by eddy fluxes originating along the northern portion of the mid-ocean ridge. It is these eddy fluxes that are primarily responsible for balancing the heat loss to the atmosphere in the interior of the sub-basins. Note that there is also a time-dependent heat flux northward along the ridge. This is a result of the seasonal correlation between the meridional velocity over the ridge (maximum shortly after cooling has ceased) and the temperature of the northward flowing water (also high after cooling has ceased).

The eddies are generated by a baroclinic conversion of mean potential energy into eddy kinetic energy (BC), and barotropic conversion from mean kinetic energy into eddy kinetic energy (BT):

$$BC = -g\gamma\overline{v'\sigma'_0}/\rho_0, \quad BT = \overline{u'v'}U_y, \quad (4)$$

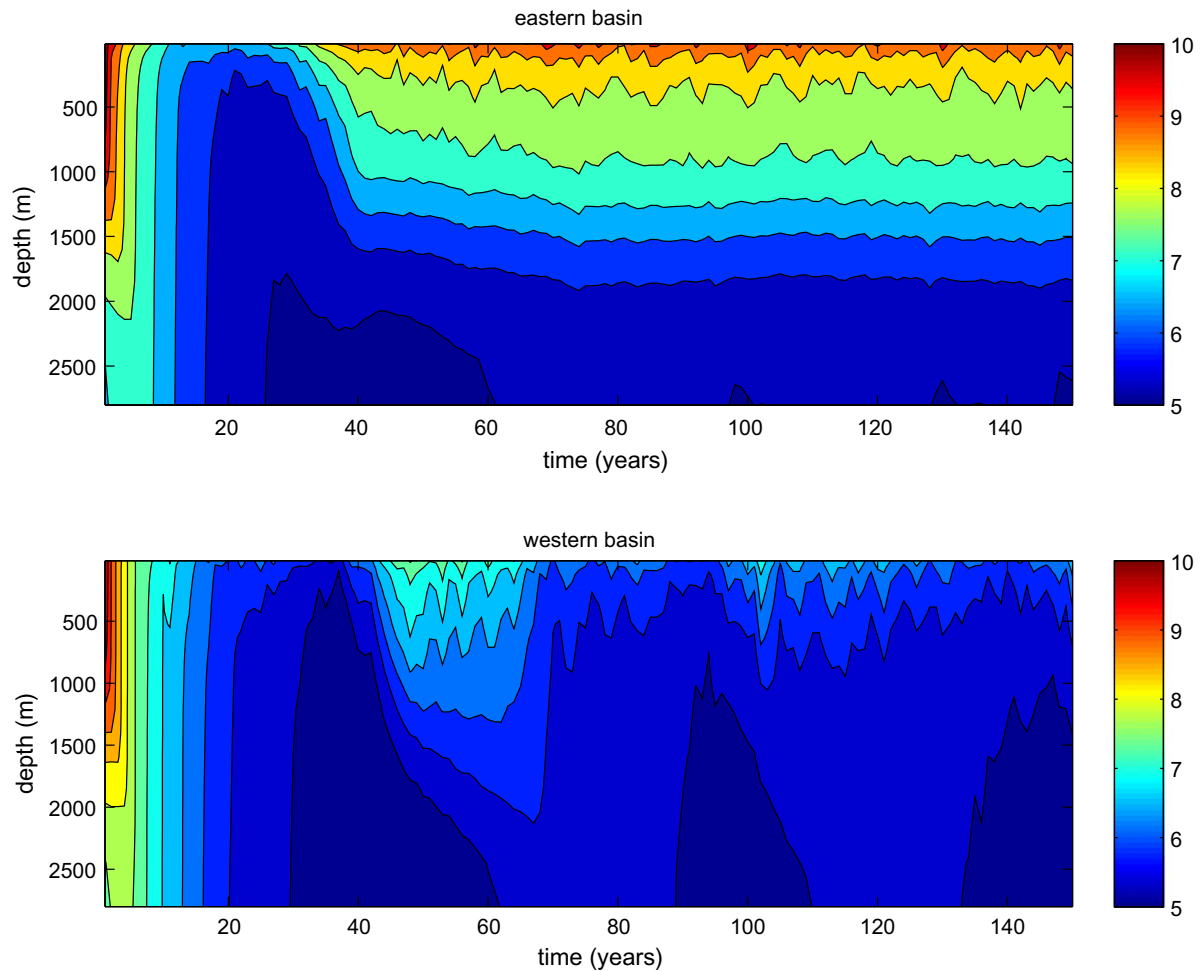


Fig. 7. Time series of annual mean temperature ($^{\circ}\text{C}$) in the central eastern basin (top) and western basin (bottom), locations are indicated in Fig. 4.

where g is the gravitational acceleration, $\gamma = \partial z / \partial y$ is the mean isopycnal slope, $\overline{v'\sigma'_0}$ is the horizontal eddy density flux across the mean isopycnal slope, $\overline{w'v'}$ is the eddy momentum flux across the mean horizontal velocity shear U_y , and ρ_0 is a reference density (Gill, 1982, p. 566). The energy conversion is dominated by the baroclinic term, shown in Fig. 11, where potential energy is extracted from the mean flow by eddies transporting density down the mean density gradient. The barotropic conversion term is an order of magnitude smaller than the baroclinic term. The regions of largest energy conversion are located along the southeastern portion of the eastern boundary and the northern portion of the mid-ocean ridge (negative values indicate eddy growth). The regions of large energy conversion are located just upstream of the regions of large eddy heat flux, confirming that the eddies are generated by baroclinic instability of the mean boundary current. The region of energy conversion along the eastern boundary is located just where the bottom topography narrows and the slope steepens, pointing to its importance in triggering the release of heat from the boundary current. The largest eddy fluxes are not found at the steepest topographic slope, as might be expected from linear theory, most likely due to the three dimensional nature of the flow and nonlinear effects (such as reduced baroclinic shear due to eddy heat fluxes). This extraction of potential energy from the baroclinic boundary current is responsible for the boundary current becoming more barotropic as it flows northward, perhaps related to the observation that the iNwAC is more barotropic than the oNwAC (Oliver and Heywood, 2003).

3. Topographic influences

The standard model configuration produces a circulation and hydrography that have many similarities with the Nordic Seas. The intent here is not to reproduce the real Nordic Seas, but to try to understand what aspects of this region are responsible for the unique circulation pattern of two northward branches of the NwAC, and the marked difference between the hydrography and convection in the Lofoten and Greenland Basins.

3.1. Eastern slope

The warmer waters and shallower mixing in the Lofoten Basin could be due to the fact that it is located on the eastern side of the Nordic Seas, where the Atlantic Water enters, and is thus more likely to be warm compared to the Greenland Sea that is further downstream from the inflow. It is also tempting to interpret the branching of the NwAC as simply a result of the bottom topography and the flow following barotropic potential vorticity contours. This is tested by using a bottom topography that is symmetric around the basin (it does not have the region of steep topography along the eastern boundary), but is otherwise identical to the standard topography. The circulation and hydrography are much more symmetric between the eastern and western basins, as shown by the vertical section in Fig. 12. There exists a strong cyclonic boundary current around the outer perimeter of the basin, and weak cyclonic circulations within both sub-basins as well. The temperature

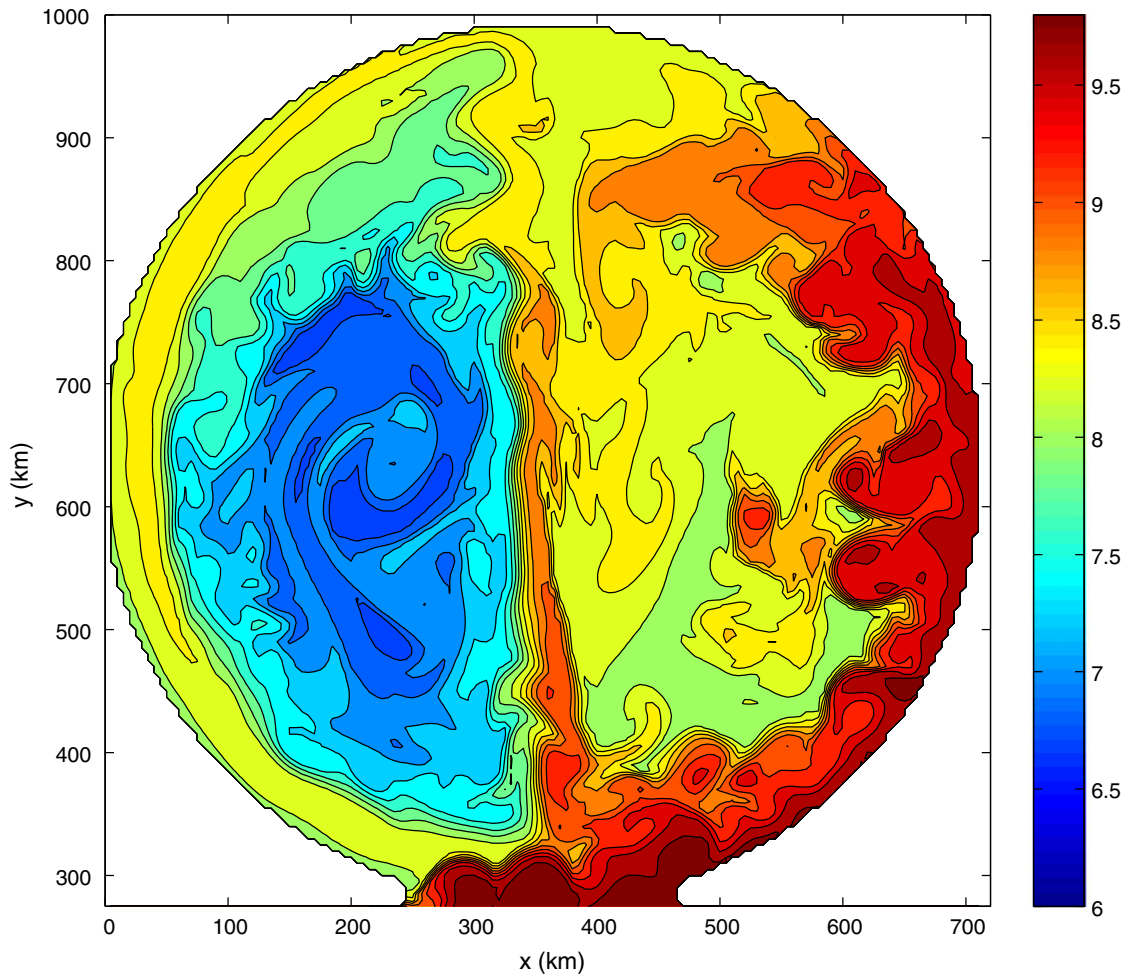


Fig. 8. Sea surface temperature ($^{\circ}\text{C}$) 80 days after cooling has ceased in year 95.

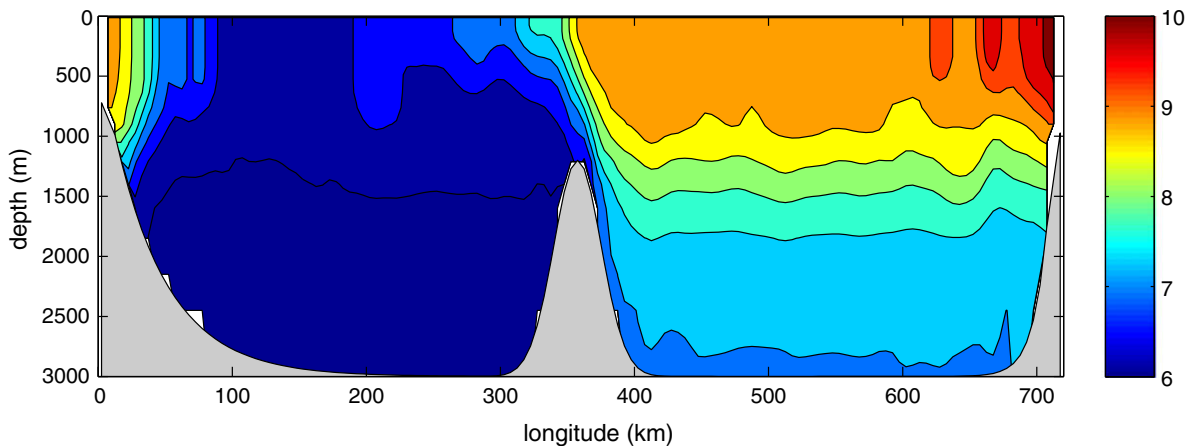


Fig. 9. Vertical section at 600 km latitude of temperature ($^{\circ}\text{C}$) on day 120 of model year 99. Dense water from the western basin is spilling over the ridge to fill the deep eastern basin.

in the eastern basin is much colder than in the case with the steep topography, and is actually colder than the temperature in the western basin, even though it is closer to the inflowing warm water.

The energy conversion and eddy heat flux terms indicate that the heat is now provided to the eastern basin interior primarily from baroclinic instability of the southward flowing current along the mid-ocean ridge, not from the eastern boundary as in the pre-

vious case. The boundary current along the eastern boundary remains strongly baroclinic because the eddies have not extracted potential energy via baroclinic instability (Fig. 12). This finding indicates that the barotropic nature of the eastern boundary current in Fig. 5 results from the upstream baroclinic instability triggered by the enhanced topographic slope along the boundary.

This result supports the interpretation that the steep topography was responsible for the enhanced eddy shedding, and that

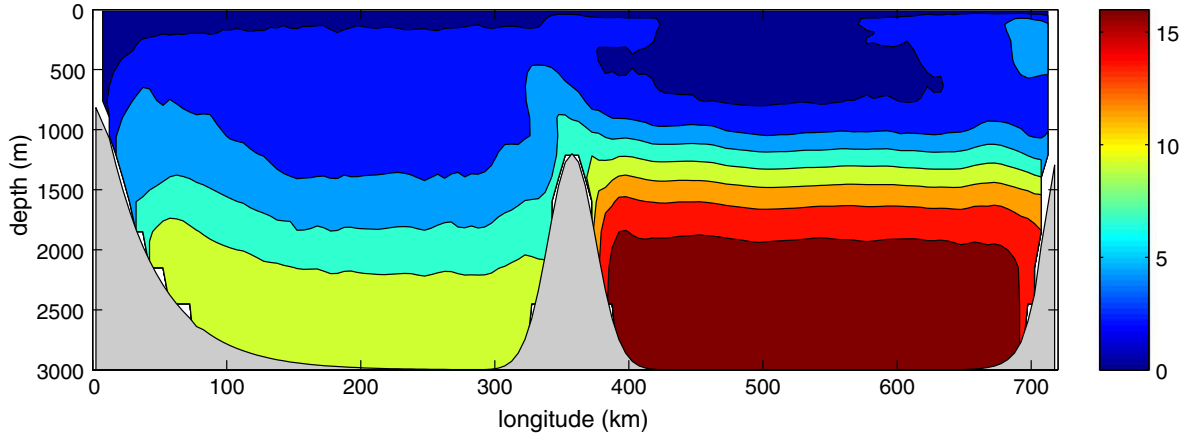


Fig. 10. Zonal section at 630 km latitude of an ideal age tracer, value set to 0 at the surface, increases linearly with time in the interior (years).

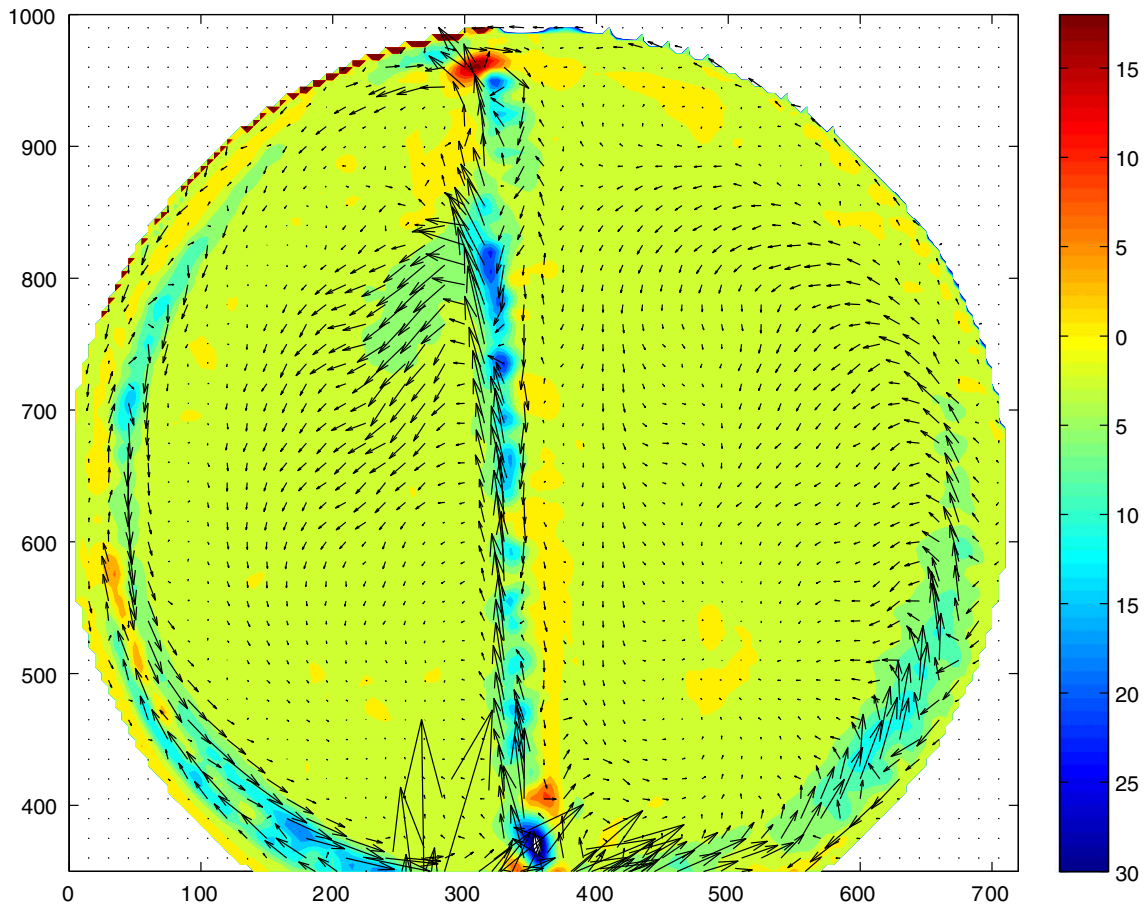


Fig. 11. Horizontal eddy temperature flux (vectors) and baroclinic conversion rate (from Eq. (4), units $10^{-8} \text{ m}^2 \text{ s}^{-3}$) at 275 m depth averaged over the final 75 years of integration.

the eddies were responsible for transporting heat from the boundary current into the interior. The proximity of the warm inflowing water to the eastern basin is not sufficient to result in a warmer eastern basin. The circulation over the ridge is now predominately southward, with only a weak northward flow along the western flank of the ridge. The ridge provides a pathway for warm water to be advected from the perimeter into the basin interior, as evidenced by the band of warm water lying over the ridge. The resulting thermal wind requires a southward flow on the eastern flank of the ridge and a northward flow on the western flank of the ridge.

This emphasizes that the northward flow in the standard case is not a direct result of the existence of the ridge. Although in both cases the flow is constrained by local topography, the direction of flow (northward or southward) is not. In order to have northward flow over the ridge, the eastern basin needs to be warm, or filled with Atlantic Water, which requires eddies to transport the warm water across the topographic contours. A calculation with a region of steep topography along the western boundary instead of the eastern boundary produces a warm western basin with a mid-depth thermocline and a southward flowing baroclinic current

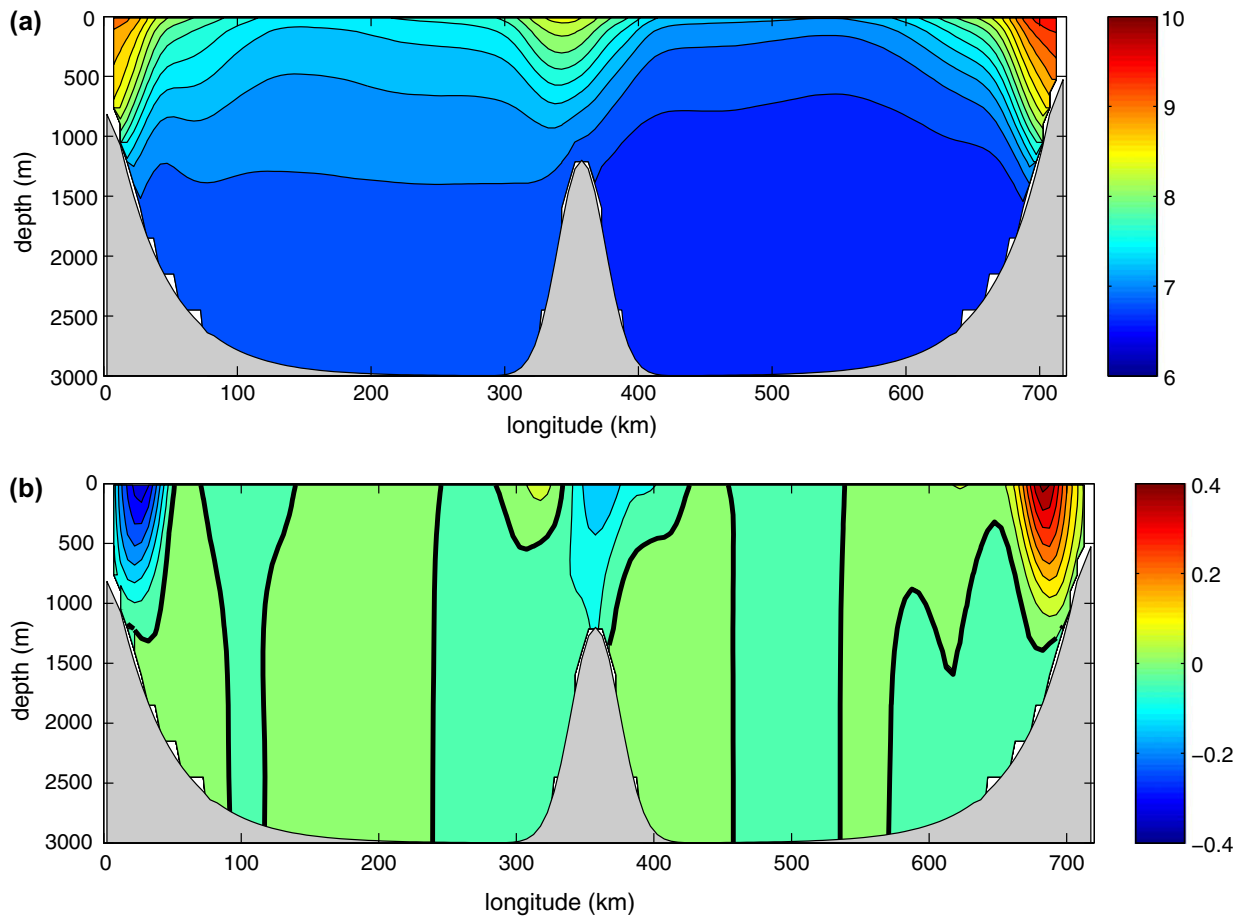


Fig. 12. Vertical section at 630 km latitude of mean (a) temperature (contour interval 0.2 °C) and (b) meridional velocity (m s^{-1} , contour interval 0.05, zero line bold) taken over the final 75 years of integration for the case without the steep topography along the eastern boundary.

over the mid-ocean ridge, nearly the mirror image of the standard case discussed in the previous section.

A calculation with steep topography all the way around the basin results in a hydrography and circulation that are similar to the standard calculation. The inflowing boundary current is sufficiently unstable (large ϵ , in the formalism of Spall (2004)) that a large amount of heat is fluxed into the eastern basin interior before it is carried around the perimeter into the western basin. This warmer eastern basin then produces the northward flow over the ridge, a colder western basin, and the mid-depth thermocline in the eastern basin. In this case, the asymmetry in eddy heat flux is not due to the bottom topography but is instead a result of the warm water entering the marginal sea on the eastern side and the eddies being able to extract a large portion of the heat content before it reaches the western basin.

3.2. Ridge shape

The warm water carried into the basin interior by eddies from the eastern boundary appears to be trapped in the eastern basin by the presence of the mid-ocean ridge. Once trapped, the thermal wind requires a northward flow over the ridge, consistent with the oNwAC. However, it turns out that the ridge shape also matters, the ridge does not simply block the eddies from propagating into the western basin. A calculation was carried out with the steep topography along the eastern boundary but with a narrow ridge of 1200 m depth (1 grid cell wide and vertical sides). Warmer water is now found in the eastern basin, as in the standard case, but now the eastern basin is colder, and the western basin is war-

mer, than in the standard case (Fig. 13). The region of weak stratification in the upper water column of the eastern basin is also less pronounced. The flow over the ridge is northwards, but is much weaker than for the case with a wide ridge. This is because the sloping ridge has a stabilizing effect on the ridge current compared to the case with vertical side walls (BG72; Spall, 2004). Even though the lateral density gradient across the narrow ridge is weaker than for the wide ridge, the resulting ridge current is more unstable and is able to flux heat into the western basin. The colder interior of the eastern basin also results in a larger horizontal density gradient across the eastern boundary current and, thus, stronger baroclinic velocities than are found for the wide ridge case.

The energy conversion rates indicate that the eastern boundary current and mid-ocean ridge current are both baroclinically unstable, much as in the central case. Heat is provided to the interior of both basins along their eastern boundaries. The resulting extraction of potential energy in the southeastern portion of the eastern boundary current results in a more barotropic eastern boundary current by the mid-latitude of the basin (Fig. 13), as also found in the central case. However, unlike the central case, this configuration does not produce a strong barotropic cyclonic circulation in the eastern basin, most likely due to the loss of closed f/h contours with the vertical ridge.

3.3. Ridge and sill depth

The standard calculation takes the depth of the sill and ridge to both be 1200 m. However, the hydrography within the marginal seas is sensitive to the depth of both the sill and the ridge.

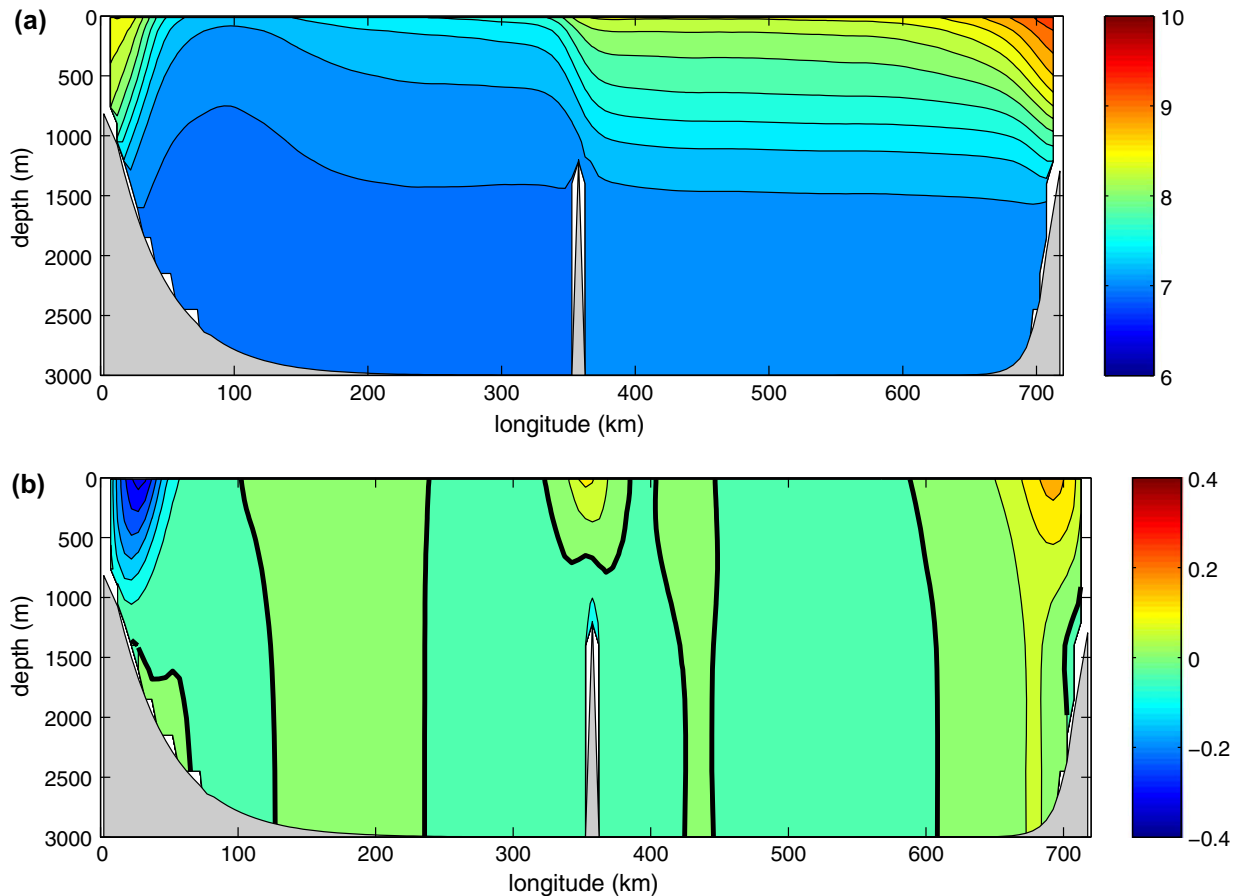


Fig. 13. Vertical section at 630 km latitude of mean (a) temperature (contour interval 0.2 °C) and (b) meridional velocity (m s^{-1} , contour interval 0.05, zero line bold) taken over the final 75 years of integration for the case with a narrow ridge.

Even for configurations that are not hydraulically controlled, changing the sill depth changes the properties of convective water masses in semi-enclosed marginal seas because it reduces both the horizontal and vertical scales over which the warm water flows into the basin (Iovino et al., 2008). For shallower sill depths, the exchange between the marginal sea and the open ocean is partially blocked and thus requires that denser waters be formed in the marginal sea in order to balance the surface heat loss. However, the boundary current is also narrower with a shallow sill because the inflowing waters are confined to those topographic contours that extend over the sill into the open ocean. As a result, the boundary current is more unstable for a given density contrast between the boundary current and the interior.

The expected trend of increasing product water density with decreasing sill depth is found for the current configuration with both a sill and a mid-basin ridge. However, the depth of convective water formation in the eastern basin also depends on the depth of the sill. A series of calculations have been carried out in which the ridge is held fixed at 1200 m depth and the sill is set to 1600 m, 800 m, and 500 m depth. The stratification in the middle of the eastern basin indicates that the calculations with decreased sill depth produce a basic hydrography similar to the standard case (Fig. 14a), although the depth that separates the convective waters from the weakly stratified abyssal waters decreases with decreasing sill depth. The upper ocean stratification increases and the minimum stratification that marks the eastern basin convective water weakens as the sill depth decreases. This indicates that the heat transported into the basin interior is largely confined to the depths less than the sill depth, consistent with the results of Iovino et al. (2008).

Qualitatively similar asymmetries between the eastern and western basins are found as long as the ridge depth is greater than the sill depth. A calculation with a 2000 m deep ridge and a 1200 m deep sill still produces a mid-depth thermocline and the two poleward currents (dotted line in Fig. 14b). Deep ridges are effective at blocking the westward transport of heat by the eddies because they have a barotropic component (owing to their baroclinic instability source), so that even relatively weak topography provides a strong barotropic potential vorticity barrier.

A different result is found when the sill depth is deeper than the ridge depth. The case with a 1600 m deep sill and 1200 m deep ridge does not produce an upper ocean convective water in the eastern basin, where instead convection penetrates all the way to the bottom (Fig. 14a). This stratification is very similar to that found in the western basin for the 1200 m deep sill. Calculations with a sill depth of 1200 m and ridge depths of 800 m and 500 m also do not produce a mid-depth thermocline in the eastern basin (the thin line in Fig. 14b is the 800 m sill case). A calculation with both sill and ridge depths of 1600 m does produce a mid-depth thermocline in the eastern basin, so this suggests that it is the relative depth of the sill compared to the ridge that is important for maintenance of the mid-depth thermocline.

Warm water is brought into the basin at depths less than the sill depth. If a mid-depth thermocline is to be supported, it must be located at or below the sill depth since the heat transported into the basin by eddies extends to the sill depth and must be balanced by convection. However, the dense water that is also required to maintain the mid-depth thermocline enters the eastern basin at the depth of the ridge crest. This dense water mixes with the ambient water in the eastern basin as it cascades down the eastern

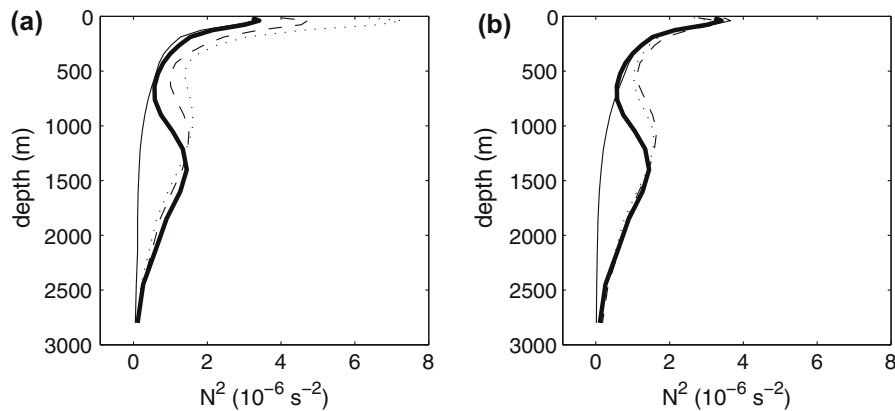


Fig. 14. Mean stratification in the center of the eastern basin for (a) ridge depth of 1200 m and sill depth of: 1200 m (bold), 800 m (dashed), 500 m (dotted), 1600 m (thin); (b) sill depth of 1200 m and ridge depth of: 1200 m (bold), 800 m (thin), 2000 m (dotted), 800 m with gaps in the ridge (dashed).

slope of the ridge (Fig. 10). In the model, this mixing is artificially enhanced because the dense water lies over lighter water as it flows down the model topography. This triggers convective mixing that would not happen if the model had sufficient vertical resolution or numerics to keep the dense water on the bottom. This mixing erodes any stratification below the depth of the ridge crest in the eastern basin. Thus, if the ridge is shallower than the sill, this entrainment removes any deep stratification. In the absence of such numerically induced mixing, this dense water could flow into the abyssal eastern basin and, if it remained on the bottom, it is expected that a thermocline below the ridge crest could be supported. Thus, it is likely that the lack of a mid-depth thermocline for those model runs here in which the sill is deeper than the ridge is a result of model numerics and not intended physics.

This is supported by a calculation with a shallow ridge (800 m), that contains three 15 km gaps located at latitudes 455 km, 635 km, and 815 km. This is probably a more realistic representation than is the solid ridge because the actual ridge system in the Nordic Seas is permeated with narrow gaps that extend well below the ridge crests. There is now exchange of dense water through the gaps without excessive mixing diluting the density of the water. A mid-depth thermocline similar to the previous cases (dashed line in Fig. 14b) is once again supported. The surface water is warmer than is found for the case with no gaps and the deep basin is approximately 1 °C colder. The warming of the near surface waters is a result of the convective mixing being confined to the upper 1000 m and the denser deep water results from enhanced exchange with the western basin.

4. Summary and conclusions

Warm, salty water masses of Atlantic origin undergo significant transformation along their pathway through the Nordic Seas. The product waters form an important component of the Atlantic Meridional Overturning Circulation, which is central to the global-scale oceanic circulation and the ocean's role in climate. Much attention has been previously paid to the region of deep convection in the central Greenland Sea, where the densest water masses are formed. However, recent studies have concluded that water mass transformation in the cyclonic boundary current system, and in the Lofoten Basin in particular, are more important for the AMOC than the region of deep convection in the Greenland Sea (Mauritzen, 1996a,b; Isachsen et al., 2007; Eldevik et al., 2009). The hydrography within the Lofoten Basin is quite different from that found in the Greenland Sea (or the Labrador Sea) and is characterized by a mid-depth thermocline at approximately 1000 m. The upper 1000 m is filled with warm, salty Atlantic waters, apparently transported from the

boundary current by mesoscale eddies (Poulain et al., 1996; Köhl, 2007). Another unique aspect of the oceanography in the Lofoten Basin is that the poleward transport is carried in two branches, one located over the continental slope and the other following the mid-ocean Mohn and Knipovich Ridge system. Despite its importance for water mass transformation and air-sea exchange, relatively little is known about the dynamics of the Lofoten Basin, or how it interacts with the adjacent Greenland Sea.

A series of numerical model calculations are applied to better understand the circulation and water mass transformation in the Nordic Seas. Although very idealized, the central model calculation produces hydrography and circulation that are in broad agreement with that found in the Lofoten and Greenland Basins. An increase in topographic slope along the eastern boundary of the eastern basin (representing the Lofoten Basin) results in increased eddy fluxes from the boundary current into the basin interior, warming the upper ocean and balancing heat loss to the atmosphere. Because of this enhanced eddy flux compared to the boundary current along the perimeter of the western basin (representing the Greenland Sea), the upper ocean in the eastern basin is warmer than the upper ocean in the western basin. The resulting thermal wind shear over the mid-ocean ridge is balanced by a poleward flowing boundary current over the ridge, consistent with the outer branch of the Norwegian Atlantic Current. Baroclinic eddy exchange over the ridge between the eastern and western basins fluxes warm waters formed in the eastern basin into the western basin, and cold waters formed in the western basin into the abyssal eastern basin. Because the western basin is colder than the eastern basin, this exchange results in a mid-depth thermocline consistent with that found in the Lofoten Basin. Model calculations indicate that the depth of the thermocline is largely controlled by the depth of the sill separating the marginal seas from the open ocean to the south.

There are two ingredients essential to producing the two poleward flowing currents and the mid-depth thermocline in the eastern basin. There must be an asymmetry in the eddy heat flux of the cyclonic boundary current that encircles both the eastern and western basins. In the cases studied here this arises as a result of steep topography along the eastern boundary, as exists in the Lofoten Basin. There must also be a means for dense water formed in the western basin to get into the eastern basin. This can be achieved either by baroclinic eddy fluxes over the ridge or by flows through deep gaps in the ridge.

There are several consequences of this distinct situation in the Lofoten Basin. The spreading of warm waters away from the boundary and over a large surface area can be expected to result in a larger heat loss to the atmosphere and water mass transformation than if these warm waters were trapped along the boundary.

This spreading is also necessary to form the mid-depth thermocline, which in turn traps the waters near the surface and isolates the deep eastern basin from direct ventilation. This warm thermocline then drives the mid-ocean poleward current (the oNwAC).

The overarching theme of these model results is that the hydrography and circulation in convective basins is to a large degree controlled by lateral eddy fluxes. The eddy fluxes are controlled by bottom topography, sometimes by features that are located far from the deep convection sites. One consequence is that regional characteristics of the bottom topography can have a dominant influence on the basin-scale flow. For example, the region of steep topography along the eastern boundary results in the anomalously warm eastern basin, which then results in the poleward flowing warm water branch over the mid-ocean ridge. The mere existence of a ridge is not sufficient to result in this poleward branch. Depending on the topography around the perimeter of the two basins, the flow over the ridge can be poleward (unstable eastern boundary current), equatorward (unstable western boundary current), or in both directions (no steep topography). The existence of an adjacent cold basin and a permeable mid-ocean ridge are also necessary for the existence of a mid-depth thermocline in the warm basin. The depth of the upstream sill also influences the depth of the thermocline by trapping the heat near the surface and altering the stability of the boundary current. The non-local aspect of the eddy fluxes and the influence of topographic slope on the stability of the boundary currents pose challenges if one is to attempt to parameterize the effect of such eddies on deep convection in the Nordic Seas or other convective basins.

Acknowledgments

This work was supported by NSF Grants OCE-0726339 and OCE-0850416. This work has benefited from many discussions with Fiamma Straneo. Comments and suggestions from two anonymous reviewers helped to clarify the discussion. Kevin Oliver and Karen Heywood are thanked for providing the CATS data in Fig. 2.

References

- Aagaard, K., Swift, J.H., Carmack, E.C., 1985. Thermohaline circulation in the Arctic Mediterranean Seas. *J. Geophys. Res.* 90, 4833–4846.
- Blindheim, J., 1990. Arctic Intermediate Water in the Norwegian Sea. *Deep-Sea Res. A* 37, 1475–1489.
- Blumsack, S.L., Gierasch, P.J., 1972. The effects of topography on baroclinic instability. *J. Atmos. Sci.* 29, 1081–1089.
- Chanut, J., Barnier, B., Large, W., Debret, L., Penduff, T., Molines, J.M., Mathiot, P., 2008. Mesoscale eddies in the Labrador Sea and their contribution to convection and restratification. *J. Phys. Oceanogr.* 38, 1617–1643.
- Cuny, J., Rhines, P.B., Niiler, P.P., Bacon, S., 2002. Labrador Sea boundary currents and the fate of the Irminger Sea Water. *J. Phys. Oceanogr.* 32, 627–647.
- Eldevik, T., Nilsen, J.E.O., Iovino, D., Olsson, K.A., Sando, A.B., Drange, H., 2009. The thermohaline circulation: overflows, sources, and observed variability 1950–2005. *Nat. Geosci.* doi:10.1038/NGEO518.
- Gill, A., 1982. *Atmosphere–Ocean Dynamics*. Academic Press, New York, p. 662.
- Iovino, D., Straneo, F., Spall, M.A., 2008. On the effect of a sill on dense water formation in a marginal sea. *J. Mar. Res.* 66, 325–345.
- Isachsen, P.E., Mauritzen, C., Svendsen, H., 2007. Dense water formation in the Nordic Seas diagnosed from sea surface buoyancy fluxes. *Deep-Sea Res.* 54, 22–41.
- Katsman, C.A., Spall, M.A., Pickart, R.S., 2004. Boundary current eddies and restratification of the Labrador Sea. *J. Phys. Oceanogr.* 34, 1967–1983.
- Killworth, P.D., 1983. Deep convection in the World Ocean. *Rev. Geophys.* 21, 1–26.
- Köhl, A., 2007. Generation and stability of a quasi-permanent vortex in the Lofoten Basin. *J. Phys. Oceanogr.* 37, 2637–2651.
- Lilly, J.M., Rhines, P.B., 2002. Coherent eddies in the Labrador Sea observed from a mooring. *J. Phys. Oceanogr.* 32, 585–598.
- Marshall, J., Schott, F., 1999. Open-ocean convection: observations, theory, and models. *Rev. Geophys.* 37, 1–64.
- Marshall, J., Hill, C., Perelman, L., Adcroft, A., 1997. Hydrostatic, quasi-hydrostatic, and nonhydrostatic ocean modeling. *J. Geophys. Res.* 102, 5733–5752.
- Mauritzen, C., 1996a. Production of dense overflow waters feeding the North Atlantic across the Greenland–Scotland Ridge. Part 1: evidence for a revised circulation scheme. *Deep-Sea Res.* 43, 769–806.
- Mauritzen, C., 1996b. Production of dense overflow waters feeding the North Atlantic across the Greenland–Scotland Ridge. Part 2: an inverse model. *Deep-Sea Res.* 43, 807–835.
- Nilsen, J.E., Falck, E., 2006. Variations of mixed layer properties in the Norwegian Sea from the period 1948–1999. *Prog. Oceanogr.* 70, 58–90.
- Oliver, K.I.C., Heywood, K.J., 2003. Heat and freshwater fluxes through the Nordic Seas. *J. Phys. Oceanogr.* 33, 1009–1026.
- Orvik, K.A., 2004. The deepening of the Atlantic Water in the Lofoten Basin of the Norwegian Sea, demonstrated using an active reduced gravity model. *Geophys. Res. Lett.* doi:10.1029/2003GL018687.
- Orvik, K.A., Niiler, P., 2002. Major pathways of Atlantic Water in the northern North Atlantic and Nordic Seas toward Arctic. *Geophys. Res. Lett.* 29. doi:10.1029/2002GL015002.
- Orvik, K.A., Skagseth, O., Mork, M., 2001. Atlantic inflow to the Nordic Seas: current structure and volume fluxes from moored current meters, VM-ADCP and SeaSoar-CTD observations, 1995–1999. *Deep-Sea Res.* 48, 937–957.
- Poulain, P.-M., Warn-Varnas, A., Niiler, P.P., 1996. Near surface circulation of the Nordic Seas as measured by Lagrangian drifters. *J. Geophys. Res.* 101, 18237–18258.
- Prater, M.D., 2002. Eddies in the Labrador Sea as observed by profiling RAFOS floats and remote sensing. *J. Phys. Oceanogr.* 32, 411–427.
- Pratt, L.J., Spall, M.A., 2008. Circulation and exchange in choked marginal sea. *J. Phys. Oceanogr.* 38, 2639–2661.
- Spall, M.A., 2004. Boundary currents and water mass transformation in marginal seas. *J. Phys. Oceanogr.* 34, 1197–1213.
- Straneo, F., 2006. On the connection between dense water formation, overturning, and poleward heat transport in a convective basin. *J. Phys. Oceanogr.* 36, 1822–1840.
- Walín, G., Broström, G., Nilsson, J., Dahl, O., 2004. Baroclinic boundary currents with downstream decreasing buoyancy: a study of an idealized Nordic Seas system. *J. Mar. Res.* 62, 517–543.
- White, M., Heywood, K., 1995. Seasonal and interannual changes in the North Atlantic subpolar gyre from Geosat and TOPEX/Poseidon altimetry. *J. Geophys. Res.* 100, 24931–24941.